

OMCVD Gold Nanoparticles Covalently Attached to Polystyrene for Biosensing Applications

Sivayini Kandeepan¹, Joseph A. Paquette², Joe B. Gilroy² and Silvia Mittler¹

¹*Department of Physics and Astronomy, ²Department of Chemistry,*

The University of Western Ontario, London, Ontario, Canada

Abstract

Remarkable developments and successes were witnessed in the fabrication and implementation of optical sensors based on localized surface plasmon resonance (LSPR) for the investigation of chemical and biological material quantities. Although there are several designs of sensors - implementing gold nanoparticles (AuNPs) and their LSPR- published, most of them are still limited to small scale research laboratory use partly due to their high cost of fabrication and the high cost of waste management. Waste management of metal NPs is, in particular, critical for solution based LSPR sensors. Sensors implementing immobilized AuNPs show decreased impact in waste management and are safe with respect to an undesired release of NPs into waste water, the environment or uptake into biological systems. In addition, one-way sensors with immobilized NPs made from polymers are mass producible, therefore less expensive and easier to handle in comparison to brittle glass sensors. We report on the reproducible fabrication of chemically stable surface immobilized AuNPs grown via organometallic chemical vapor deposition (OMCVD) on a polymer substrate, namely polystyrene (PS). Oxygen plasma treated and UV ozone treated polystyrene samples depict enhanced amounts of polar –OH groups allowing for nucleation and growth of AuNPs. The optimum plasma treatment conditions, the largest shifts in the LSPR curves and the bulk sensitivity of the OMCVD grown AuNPs are discussed.

Introduction

Over the last decade, localized surface plasmon resonance (LSPR) sensing has been demonstrated to be an exceedingly powerful and quantitative probe in biomedical applications^[1]. LSPR is the resonant oscillation of conduction electrons in a confined metal surrounded by a dielectric material stimulated by incident light. For sensing and detecting purposes, gold nanoparticles (AuNPs) are the most extensively used NPs due to their unique tunable optical properties, low toxicity, chemical stability and their amenability of synthesis and functionalization^[2]. Also the LSPR frequency of AuNPs up to 10s of nm lies in the visible region, conveniently allowing the use of standard UV-Vis absorption spectroscopy for characterization and sensor performance. These sensors can be described as a type of surface-sensitive refractometer that is often used in label-free biosensing for direct detection of molecular adsorption that occurs within the immediate vicinity of a sensor surface. Small changes in the index of refraction along the surface of the sensor manifest a relatively large change in the LSPR wavelength in an absorption spectrum^[3]. Therefore, LSPR does not require additional chemical modification steps, such as fluorescence labeling.

In surface-sensitive LSPR biosensors, one of the interacting biomolecule is immobilized on the NP surface and its interaction with its biospecific partner is observed through the shift in the resonance position or by monitoring the appearance of a cross-talk peak^[4,5]. Only alterations in the refractive index architecture near the NP surface are sensed as the LSPR is only sensitive to the medium within roughly one wavelength (wavelength of the LSPR) distance from the surface^[6]. For visible light, only changes in refractive index occurring at distances within ~200 nm of the particle surface cause sufficient changes in the optical properties of the nanoparticles^[7,8]. Most LSPR biosensor systems are either solution based or fabricated on glass chips which are brittle and therefore easy to break. This drawback can be overcome by using sensor chips fabricated on transparent polymers. Polymer devices are also mass producible and will decrease the overall cost of these sensors.

Organometallic chemical vapor deposition (OMCVD) is a versatile process in which organometallic gas-phase molecules are decomposed to reactive species, leading to thin films and nanostructures of metals on functionalized surfaces^[9]. Therefore, this process can be used to fabricate AuNPs on a substrate for sensing purposes. The main advantages of OMCVD over physical vapor deposition (PVD) techniques, such as sputtering or evaporation, are the ability to

controllably create films of widely varying stoichiometry and to uniformly deposit materials selectively on so-called growth areas with reactive functional groups^[10,11]. The principle of an OMCVD process is to vaporize a metal-containing organic precursor, an organometallic complex, at relatively low temperatures and reduced pressure, and to decompose the precursor to deposit the metal either as a layer or as NPs on a functionalized substrate^[12]. By carefully controlling the functionalization on the substrate, the deposition parameters, such as the temperature and the reaction period, metallic NPs can be formed at a desired size and density on a surface. Volatile by-products are removed from the surface and diffuse into the low pressure reaction chamber. Since the metal NPs are covalently bonded to the functionalized surface, these particles are not environmentally challenging unlike in electrostatic bonding. Also when comparing with colloidal particles prepared by wet chemical methods, the OMCVD grown particles do not need any stabilization agents to control particle aggregation^[13]. Therefore, the OMCVD process is a fast, simple and economical method to obtain safe and controlled deposits of high quality metal NPs or hybrid NPs. This has been demonstrated by Palgrave et al. and Binions et al. with advances CVD methods^[14-17].

We show for the first time the fabrication of chemically stable, surface immobilized AuNPs on polystyrene (PS) substrates using an OMCVD process. In the future, this will allow an inexpensive mass fabrication of AuNP-carrying polymers samples: from solid substrates to flexible foils. The AuNPs can be grown for bio-sensing on an all-optical-all-polymer-lab-on-a-chip implementing integrated optics.

Previously surface-immobilized AuNPs were grown on thiol-terminated and amine-terminated glass surfaces using a simple OMCVD procedure^[18,19]. It has turned out that thiol-terminated surfaces generate chemically instable AuNPs which detach when brought in contact with a solvent. This lead to irreversible false sensor signals due to undesired AuNP clustering on the thiolated surface. The polar amine-termination, on the other hand, delivered chemically stable, well immobilized AuNPs with excellent sensor response^[19]. Ertorer *et al.*^[19] have used the sparsely available polar –NH groups of a monolayer of hexamethyldisilazane (HMDS) covalently attached to glass substrates to nucleate and grow stable AuNPs with the methyl(trimethylphosphine)gold(I) (CH₃)₃PAuCH₃ precursor. Therefore, initially we had chosen transparent polymers with high refractive indices carrying amine groups (Trogamid, Nylon 66 and polyacrylamide). However, the OMCVD process on these amine containing polymers was

unsuccessful. No AuNPs were deposited onto surfaces of spincoated, but untreated films of these polymers. There are several reasons for the failure: The available amine groups were not exposed to the surface. The number of amine (NH_2) groups was too low, or simply, the amine groups do not nucleate the Au from the precursor. In a new strategy we utilized the polar nature of hydroxyl (OH) groups. OH groups were a good candidate as an alternative polar nucleation site for the AuNPs. In order to test this, glass slides were oxygen plasma treated to create OH groups at the surface and AuNP were grown via OMCVD. This worked excellently, as demonstrated by strong LSPR peaks; AuNPs grew with the polar free OH groups serving as the nucleation sites. Therefore a transparent polymer, PS, was spin coated on glass substrates and exposed to oxygen plasma or UV ozone to create OH groups for nucleation. The OMCVD process was performed on these substrates and absorption spectra of the AuNP grown samples were obtained. Further the chemical stability and the bulk-sensing capabilities of the OMCVD grown nanoparticles were tested. The effects of the oxygen plasma and UV ozone treatment on the PS surface chemistry were investigated.

Results and Discussion

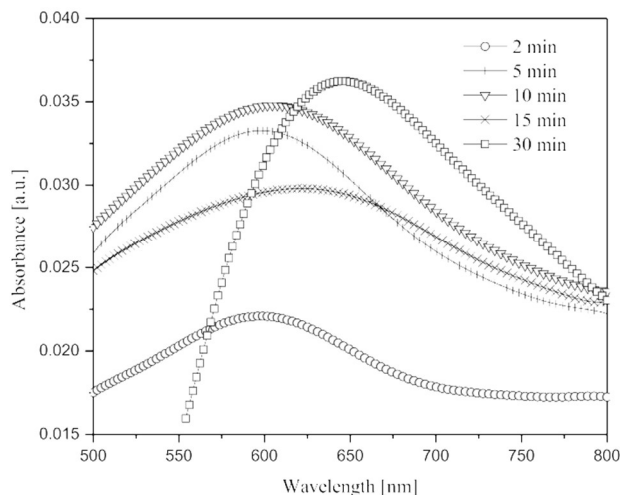


Fig. 1 UV-Vis absorption spectra of ethanol rinsed AuNPs fabricated via 20 min OMCVD (77 °C, 6 Pa) on PS treated with different oxygen plasma times.

Fig. 1 shows absorption spectra of ethanol rinsed AuNP samples on PS treated with different oxygen plasma treatment times. (The oxygen plasma treatment was performed on the PS before NP deposition, while the ethanol rinse was done after NP deposition). The OMCVD process was performed identical on all samples at 77 °C and 6 Pa for 20 min. The occurring LSPR peaks shifted from 525 to 650 nm (λ_{\max}) with increasing oxygen plasma time (2 to 30 min) as shown in Fig. 2.

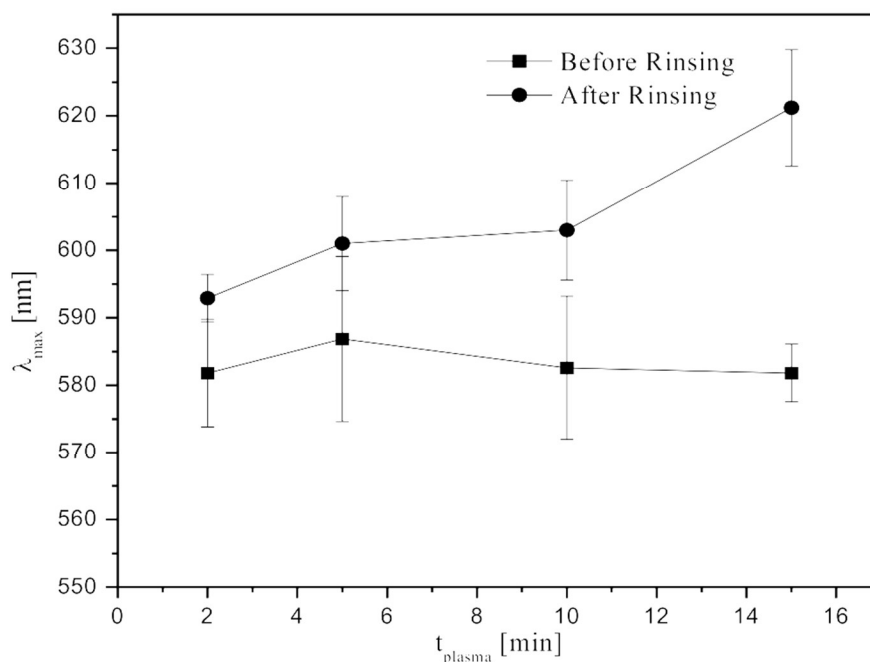


Fig. 2 UV-Vis absorption peak position (λ_{\max}) of AuNPs on PS versus oxygen plasma time.

Fig. 2 also depicts the LSPR peak position of the samples before rinsing. The ethanol rinsed samples show a clear peak shift to higher wavelength with increasing plasma treatment time whereas the as-prepared samples show a “stable” peak position at 585 ± 10 nm. The peak shift of the rinsed samples indicated an increase in the size of chemically stable AuNPs with increasing plasma time. Fig.3 depicts a scanning electron microscopy image of OMCVD grown AuNPs on polystyrene to confirm the absorption data.

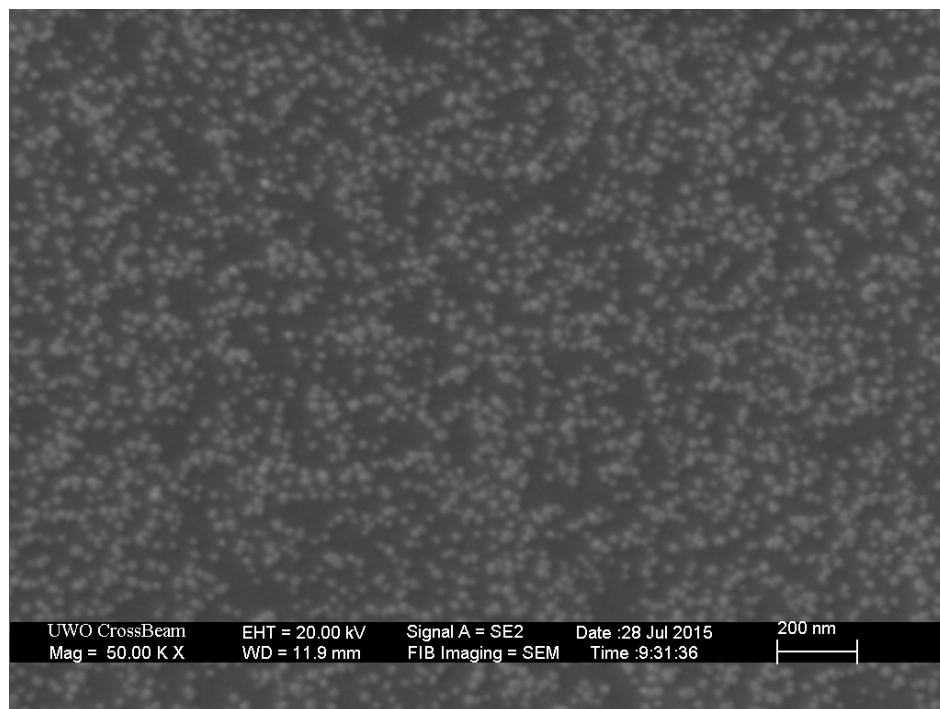


Fig. 3 SEM image of AuNPs OMCVD grown on polystyrene (2 min UV ozone, 17 min OMCVD at 6 Pa and 77 °C).

Fig. 4 shows the full width at half maximum (FWHM) of the LSPR peaks versus plasma treatment duration. The FWHM increased with plasma time for both sample sets steadily within the first 5 min from 140 ± 25 nm and 155 ± 25 nm to 185 ± 25 nm, for the before and after rinsing, respectively and then stabilized at 185 ± 25 nm. The position of the LSPR and the FWHM delivered a consistent picture: as the plasma treatment time is increased, firstly existing NPs grew larger and aggregated, increasing the FWHM and shifting the peak position. In addition, newly grown NPs contributed to the peak position and width.

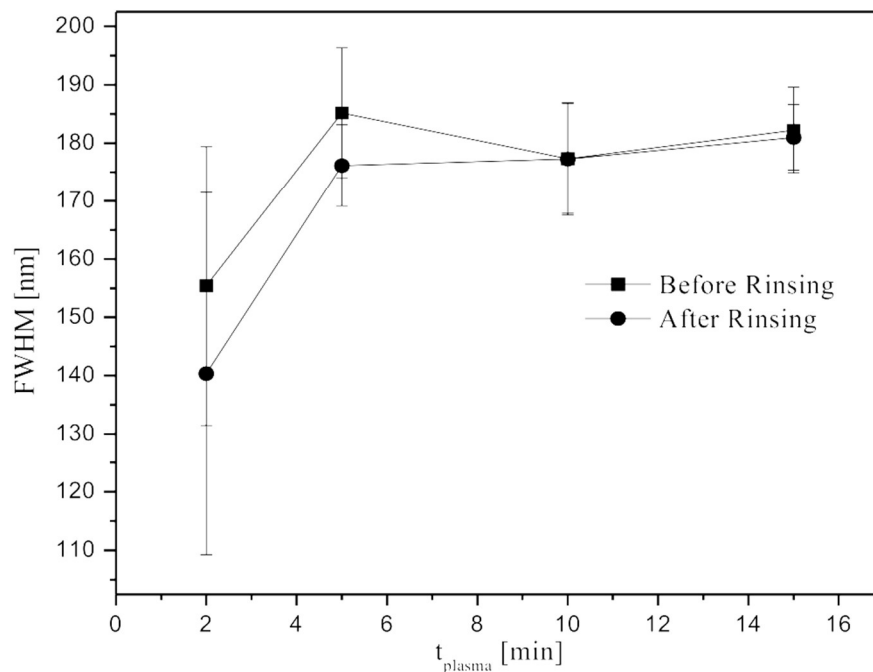
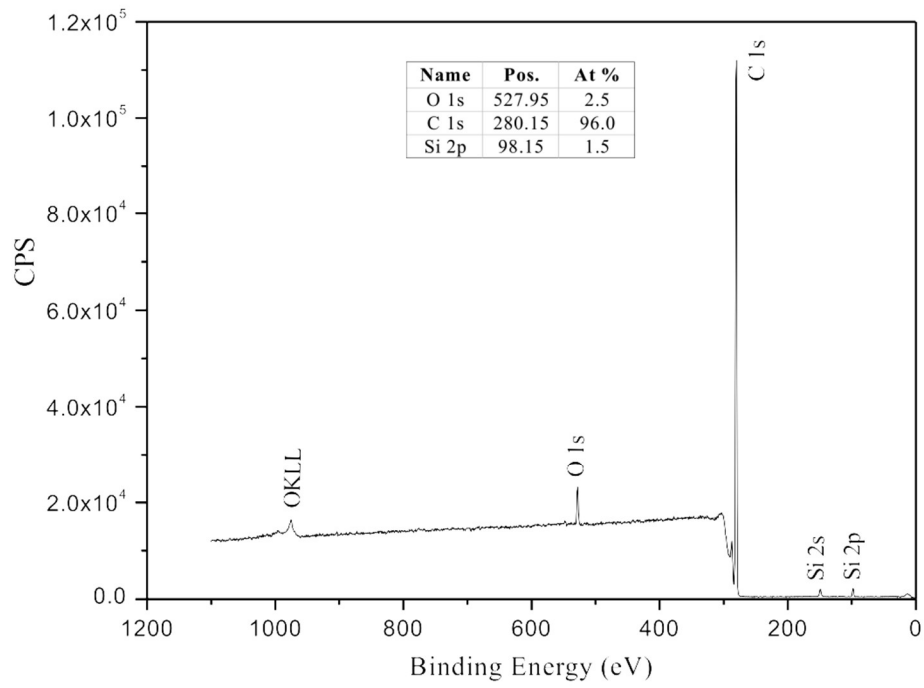
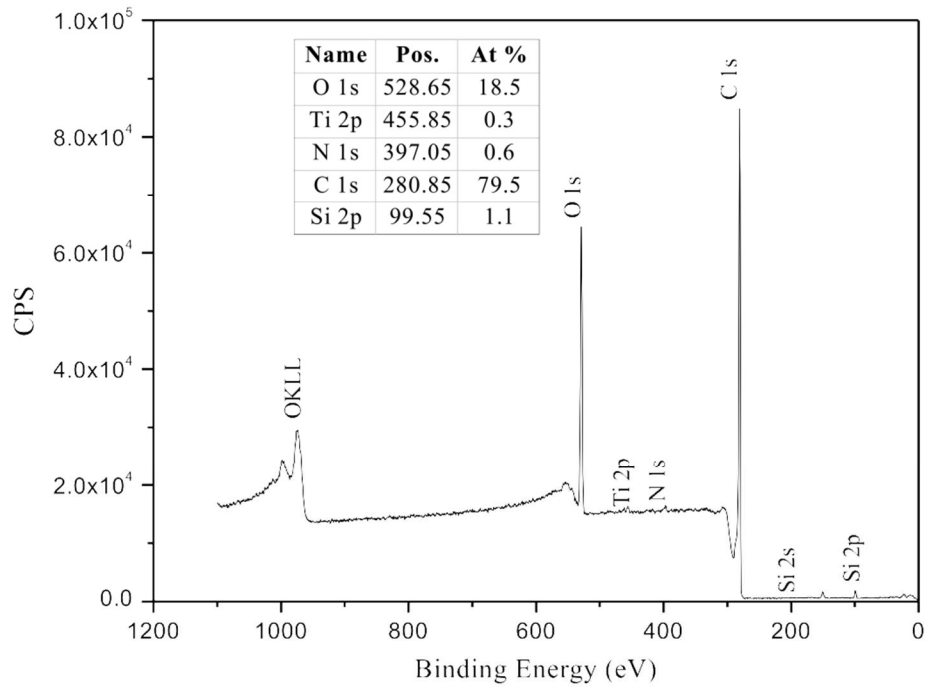


Fig. 4 FWHM of LSPR peaks of rinsed and non-rinsed AuNPs on PS versus oxygen plasma time.

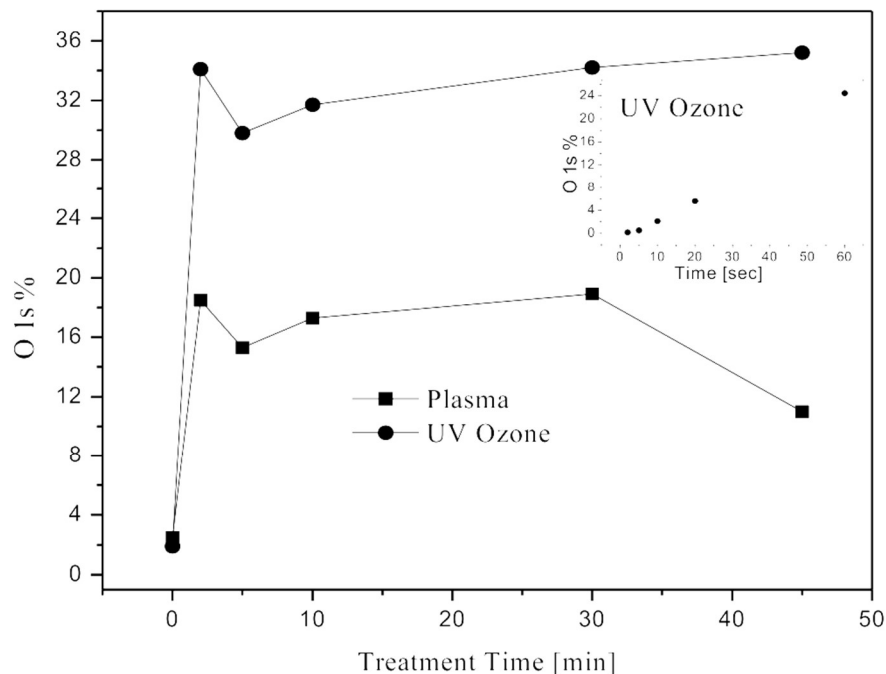
Rinsing removed loose particles of all kinds: small newly nucleated and larger particles; rinsing also removed some NP clusters. The hypothesis is that with increasing oxygen plasma times the amount of nucleation sites on the polymer surface increases, allowing for a fixed growth time, more NPs to grow and also the formation of larger nanoparticles. Not only is the peak position important in sensing but also the precision with which the peak position can be determined. This precision is directly related to the peak width. Therefore, low plasma treatment durations on the order of 2 min would be suitable to grow AuNPs followed by an extensive rinsing with ethanol to construct a chemically stable and precise sensor platform for bio-sensing purposes. The same experiments were carried out with UV ozone plasma treated PS samples. The results were comparable to the oxygen plasma treated samples.



a



b



c

Fig. 5 XPS survey spectra of PS spin coated films: a) untreated, b) treated with 2 min oxygen plasma, and c) O 1s peak height versus oxygen and UV ozone plasma time. The inset shows the first 60 s for the UV ozone treatment.

In order to test the hypothesis on an increased number of OH nucleation sites on the polymer surface with increased oxygen and UV ozone treatment time, XPS spectroscopy was performed^[20]. Fig. 5 show XPS survey spectra of an untreated PS sample (Fig. 5a) and after 2 min of oxygen plasma treatment (Fig. 5b) at the same scale. Comparing both spectra, we note an increased O 1s peak (18.5 %) in the plasma treated PS in comparison to the 2.5% for the untreated PS. Exposure to the oxygen plasma has led to the incorporation of oxygen into the PS surface within the first 2 min of plasma treatment. Fig. 5c shows the O1s peak height versus plasma treatment time for both oxygen and UV ozone treatment. Since the UV ozone plasma treatment time can be tuned finely, XPS data were obtained also from 0–2 min. These data are depicted in the inset of Fig. 5c. The amount of oxygen on the PS surface increases rapidly within the first 2 min of plasma treatment for both kinds of plasma but saturates depending on the

plasma: at ~16% for oxygen and at ~ 32% for the ozone plasma. For higher treatment times (45 min), the oxygen level decreases. It was evident that the ozone plasma treatment yielded higher oxygen concentrations than the oxygen plasma treatment for PS spin coated samples at a given treatment time and therefore providing more nucleation sites for AuNPs to grow. In addition the timing of the plasma treatment is easier to adjust. Therefore the ozone plasma treatment is the more suitable process to create OH groups in a controllable fashion on the PS sample for the fabrication of AuNPs.

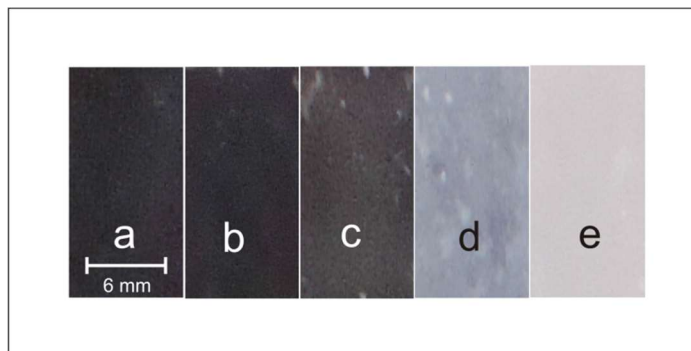
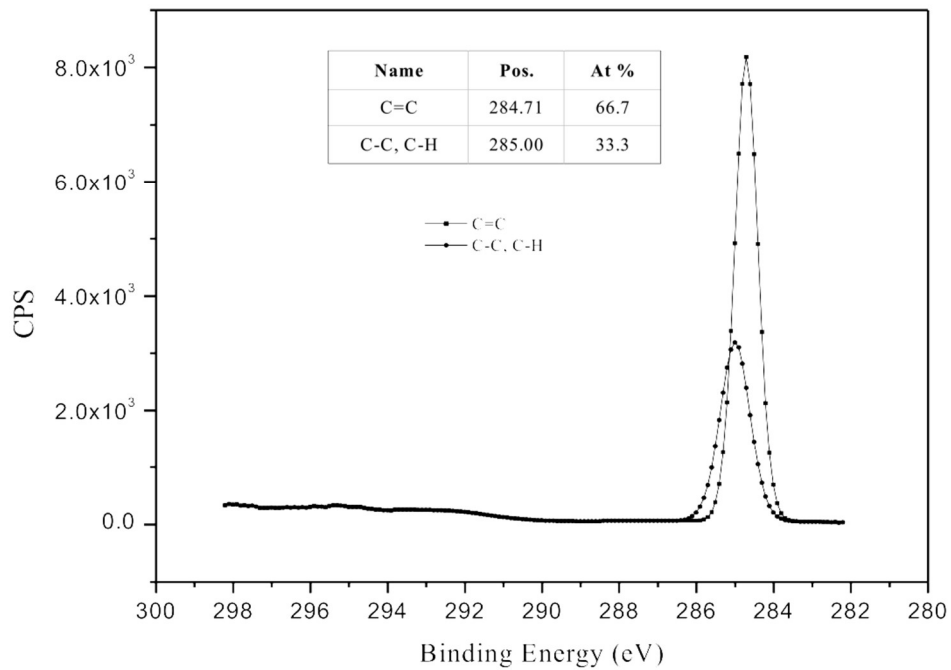


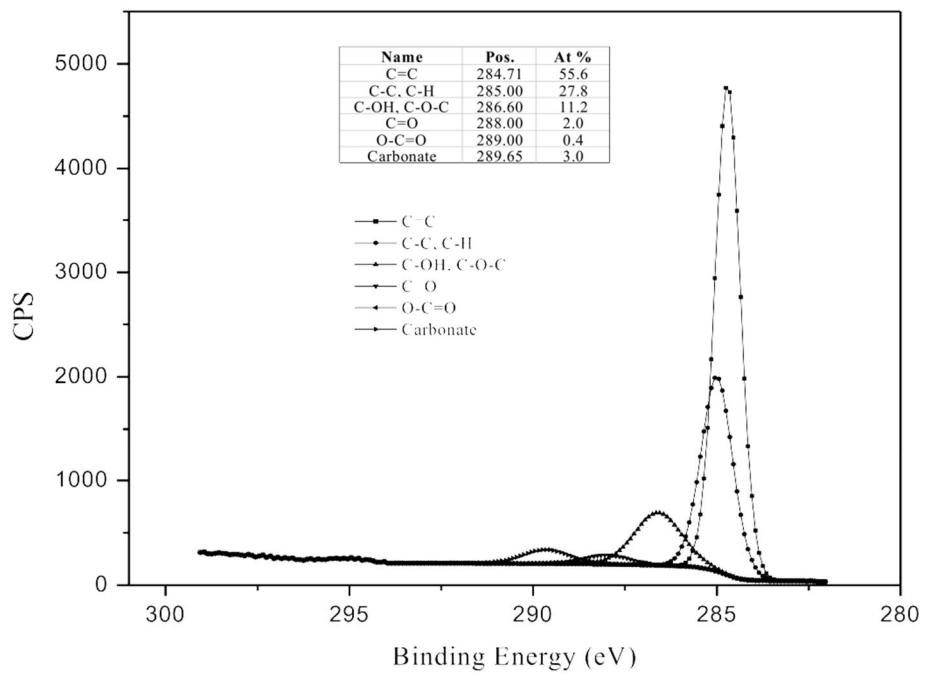
Fig. 6 PS spin coated samples treated with increasing oxygen plasma time. From left to right: 0, 5, 10, 30, 45 min.

The oxygen plasma treatment for longer duration ($t > 30$ min) alters the transparency of the PS thin films substantially. The transparent spin coated films turn into a milky white coating as shown in Fig. 6 (from left to right: 0, 5, 10, 30, 45 min treatment time) which will not be suitable for an absorption spectrum-based biosensing device. Similarly the ozone plasma treated samples turned to slightly yellowish color for longer treatment times which would lead to undesired additional absorption features in the absorption spectra.

To monitor the oxide composition, high-resolution XPS was employed on the C 1s and O 1s regions. Fig. 7 shows XPS C1s high-resolution spectra for untreated (Fig. 7a) and 2 min oxygen plasma treated (Fig. 7b) PS samples. Line fitting of the XPS C-1s peaks showed that most oxygen was introduced in the form of O-H groups (286.0 eV) but also some carbonyl (C=O) groups (288.0 eV) and ester (O-C=O) groups (289.0 eV) were present²⁰.



a



b

Fig. 7 High resolution C 1s XPS spectrum of PS; a) before and b) after 2 min exposure to oxygen plasma treatment.

The O 1s high-resolution spectrum for the 2 min oxygen plasma treated sample (Fig. 8) confirms the presence of oxygen in the form of C=O, and ether groups (C-O-C and O-C-O).

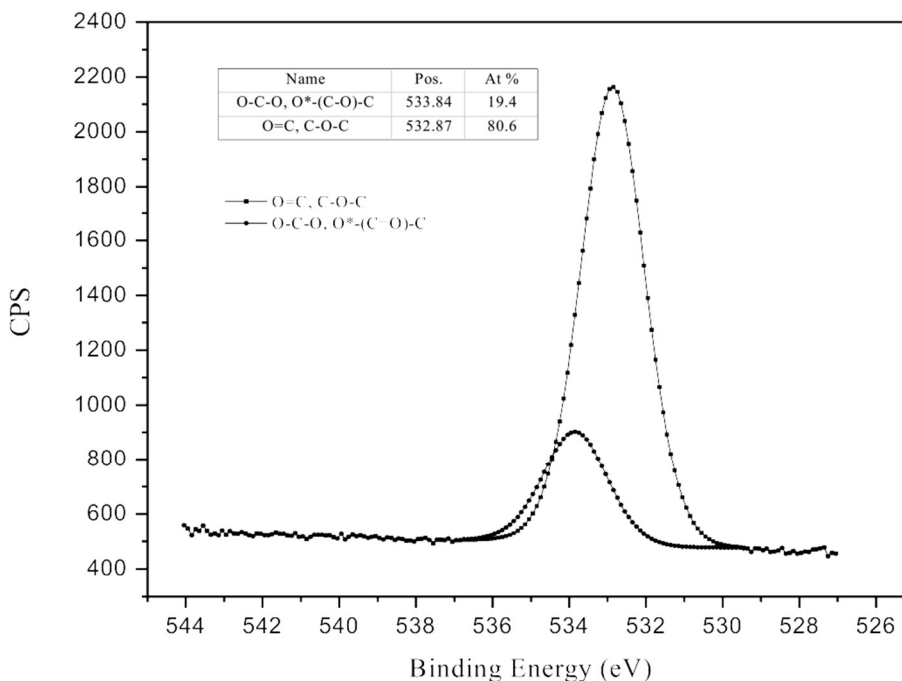
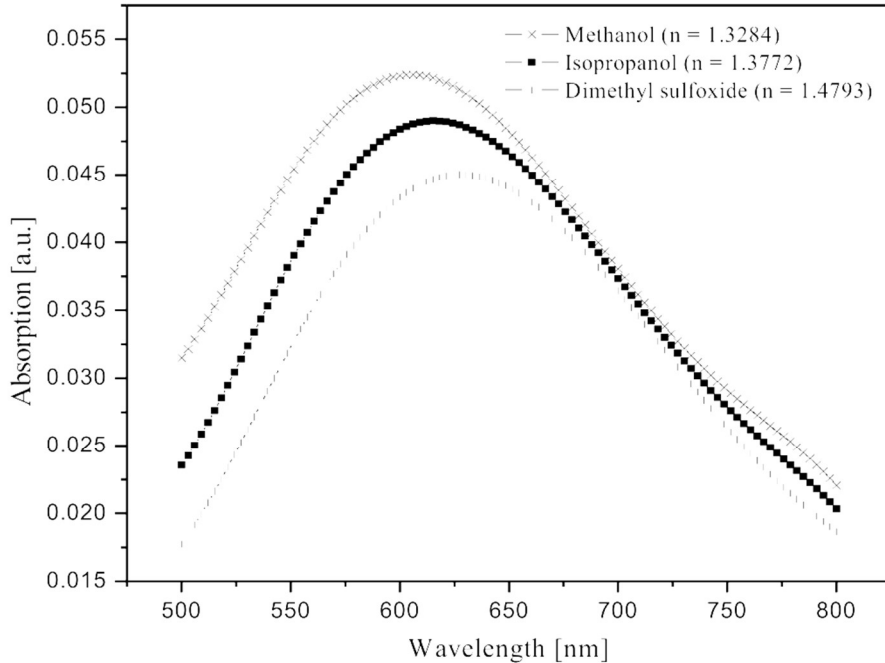


Fig. 8 High resolution O 1s XPS spectrum of PS after 2 min exposure to oxygen plasma treatment.

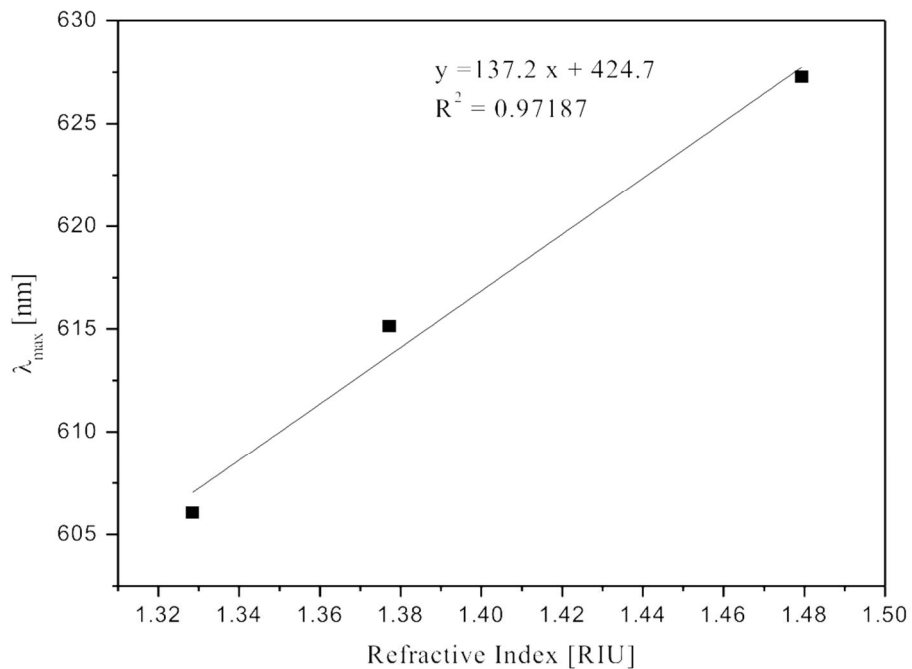
The XPS investigation showed that with increasing plasma treatment time, beyond 2 min, no additional nucleation sites were created. The LSPR position of the non-rinsed, as grown, AuNPs confirmed this behaviour. The eradication of the weakly bound Au however leads to AuNP populations with increasing diameters as the LSPR shifts to higher wavelength. The hypothesis is indirectly confirmed. A plasma treatment time around 2 min was found as the optimum to grow OMCVD AuNPs with respect to FWHM and PS “optical quality”.

Fig. 9a illustrates the LSPR spectra of a bulk sensing experiment to determine the Figure of Merit (FOM) for bulk sensing using 2 min of oxygen plasma treatment and a 20 min OMCVD

process. The spectral position of the AuNP LSPR peaks (λ_{\max}) immersed in methanol ($n = 1.3284$), isopropanol ($n = 1.3772$) and dimethylsulfoxide ($n = 1.4793$) were 606.06 nm, 615.15 nm and 627.27 nm, respectively. The λ_{\max} shifts systematically to longer wavelengths with increasing solvent refractive index (RIU) in a linear fashion in this refractive index regime. Once the AuNP substrate is immersed in a high refractive index solution, it polarizes the medium quickly and thus less energy is needed to resonate the AuNPs^[21]. Therefore the LSPR peak shifts to higher wavelengths. The gradient of the linear fit, delivering the FOM, to the λ_{\max} versus refractive index of the media data reveals the nanoparticle sensitivity (m). This linear relationship is described as $\Delta\lambda_{\max} = mn$, where $\Delta\lambda_{\max}$ is the shift in the LSPR peak position and n is the refractive index of the surrounding medium^[22]. The FOM for the 20 min OMCVD grown AuNPs for 2 min oxygen plasma treated PS substrates was $\sim 137.2 \pm 16.4$ nm/RIU (Fig. 9b). This FOM is almost 40% higher than the previously reported value on OMCVD grown AuNPs on -NH functionalized glass substrates^[23].



a



b

Fig. 9 (a) UV-Vis absorption spectra of AuNPs on PS (oxygen plasma time: 2 min) immersed in various solvents with different refractive indices. (b) LSPR peak spectral position versus refractive index of the solvents. The slope delivers the Figure of Merit for bulk sensing.

Conclusion and Future Work

OMCVD is a simple and inexpensive method to fabricate chemically stable, immobilized AuNPs with an acceptable size distribution, delivering a LSPR with an acceptable FWHM of 140 ± 25 nm. Surface immobilized AuNPs are not environmentally challenging, since they are covalently bonded to the substrate allowing for uncomplicated waste management. It is now possible to reproducibly grow chemically stable AuNPs on oxygen plasma and UV ozone treated PS. Sensors made from polymers are easy to handle, less expensive to manufacture and mass producible. XPS data and the FWHM of the LSPR curves revealed that the optimum treatment time is 2 min. An ethanol rinsing procedure was necessary to remove loose and unbound AuNPs. A higher FOM for bulk sensing was achieved in comparison to previously reported values on OMCVD grown AuNPs on glass. The question about the detailed reaction mechanism of Au

nucleation onto the polar OH groups is not the scope of this work. However, Ertorer et al.^[19] have assumed a mechanism for polar NH groups which might be similar to the OH case. Future work will focus on oxygen plasma treatment of other transparent, high refractive index materials and to implement the strategy into all-optical-all-polymer-lab-on-a-chip.

Acknowledgements

The authors would like to thank Dr. Erden Ertorer for valuable discussions. We thank the Western Nanofabrication Facility for access to the oxygen plasma treatment and the UV ozone cleaner. Surface Science Western is thanked for their help in collecting XPS data. We gratefully acknowledge the financial support provided by NSERC.

Experimental Section

Preparation of AuNP-decorated PS films

Fisher brand glass slides (8 mm x 15 mm) were cleaned in 10 min ultra-sonication bath in acetone, isopropanol and abundant amounts of ultrapure water. Then the glass slides were blown dry with nitrogen and placed for 20 min in an STS Reactive Ion Etch system (STS RIE 320 PC, Surface Technology Systems, Newport, UK; 90 W) operating under oxygen gas. Typically this method is used for cleaning and to increase the hydrophilicity of glass slide surfaces making them more suitable for spin coating photoresist or other polymers^[24]. The PS solution was prepared by dissolving 5 g of PS granulates (Nominal Granule Size 3.5 mm, Goodfellow) in 15 ml chlorobenzene (anhydrous 99.8%, Sigma Aldrich) and allowing the solution to be stirred for several days assuring complete dissolution. The polystyrene solution was pipetted on the plasma treated glass slides and spun with 3000 rpm for 1 min in a spin coater (Headway Research, Inc.). This was followed by baking the spin coated samples in an oven for 2 hours at 90 °C under atmospheric conditions to eliminate residual solvent. The polystyrene substrates were also exposed to oxygen plasma or UV ozone treatment at room temperature (Sameo UV-1, SAMEO Inc., Kyoto, Japan) for different times creating OH functionalities. Contact angle measurements were performed with Rame-Hart, Model 200 Goniometer, Rame-Hart Co. NJ, USA). The contact angle found for the plasma treated and UV ozone treated samples were $\theta < 10^\circ$ confirming the hydrophilic nature of 2 min oxygen plasma treated samples compared with the untreated samples at $\theta = 93.5^\circ \pm 0.9^\circ$.

The inner surface of the OMCVD reaction chamber was functionalized with octadecyltrichlorosilane (OTS, Sigma Aldrich, assay $\geq 90\%$), delivering a $-\text{CH}_3$ terminated surface which is a non-growth surface for the used Au precursor^[25]. This was achieved by filling the glass vessel with OTS dissolved in toluene^[21]. The introduction of a non-growth surface in the reactor increases the efficiency of AuNP growth on the functionalized substrates^[26]. Details of the OTS functionalization is described elsewhere^[15,25]. For the OMCVD process the OH functionalized PS samples and 20 mg of the gold precursor methyl(trimethylphosphine)gold(I) (see below for preparation) in a watch glass were placed on the flat bottom inside the chamber. The chamber was evacuated to 6 Pa and was positioned in a Si oil bath for 20 min which was preheated to 77 °C. This allowed the precursor to decompose and the AuNPs to nucleate and grow on the OH functionalized substrates. After AuNP growth the samples were removed from the chamber and absorption spectra were obtained using a Lambda 850 UV-VIS spectrophotometer (PerkinElmer, CA, USA) with a plain PS spin coated samples as reference. The stability of the AuNPs was tested by repeatedly rinsing the samples in anhydrous ethanol (J.T. Baker, reagent grade 95.4%) and obtaining absorption spectra afterwards. All chemicals were used without further purification.

The surface composition and functionality of the PS samples before and after oxygen and UV ozone treatments were investigated using X-ray photoelectron spectroscopy (XPS) (Kratos AXIS Ultra spectrometer) survey spectra as well as high resolution C 1s and O 1s peaks. The bulk NP sensitivity can be determined by systematically changing the refractive index of the environment for example by changing the ambient solvent. Therefore, the bulk sensing capabilities of the AuNPs were obtained by immersing the samples in different solvents such as methanol (Bio Shop, Canada, Reagent grade, anhydrous 99.8%) isopropanol (Sigma Aldrich, anhydrous 99.5%) and dimethylsulfoxide (Sigma Aldrich, 99.9%) and analyzing the shift in peak wavelength (λ_{max}) of the absorption spectra.

Preparation of methyl(trimethylphosphine)gold(I)

All reagents were purchased from Sigma Aldrich and used as supplied. Standard Schlenk techniques were employed and all manipulations were performed under an inert atmosphere. According to a modified literature procedure^[27], 1.6 M methyl lithium in diethyl ether (2.38 ml, 3.8 mmol) was added to a stirred suspension of chloro(trimethylphosphine)gold(I) (0.98 g, 3.2 mmol) in 30 ml freshly distilled and degassed diethyl ether that had been cooled to -10 °C. Upon

addition the reaction mixture turned bright yellow. The mixture was stirred for 30 min at $-10\text{ }^{\circ}\text{C}$ followed by 2 h at room temperature at which time it was colourless. The reaction mixture was then immersed in an ice bath and 40 ml of deionized and degassed water was added. The product was extracted with degassed diethyl ether ($5 \times 20\text{ ml}$) and the combined organic phases were dried with magnesium sulfate and filtered. The solvent was removed *in vacuo* to afford a light grey powder. Sublimation was performed under vacuum at $35\text{ }^{\circ}\text{C}$ and methyl(trimethylphosphane)gold(I) was isolated as a white microcrystalline solid in a yield of 0.70 g (2.4 mmol, 77%) and stored in the absence of light at $4\text{ }^{\circ}\text{C}$ under a nitrogen atmosphere. ^1H NMR (399.8 MHz, CDCl_3): δ 1.44 (d, 9H, $^3J_{\text{HH}} = 9\text{ Hz}$), 0.34 (d, 3H, $^3J_{\text{HH}} = 8\text{ Hz}$). ^{31}P NMR (161.8 MHz, CDCl_3): δ 13.34 (s). These data are consistent with previously reported values^[27].

References

- [1] J. Homola, S.Y. Sinclair, G. Gauglitz, *Sens. Actuators, B* **1999**, *54*, 3.
- [2] S. Zeng, K. Yong, I. Roy, X. Dinh, X. Yu, F. Luan, *Plasmonics* **2011**, *6*, 491.
- [3] K.S. Johnston, K.S. Booksh, T.M. Chinowsky, S.S. Yee, *Sens. Actuators, B* **1999**, *54*, 80.
- [4] P. Rooney, S. Xu, A. Rezaee, T. Manifar, A. Hassanzadeh, G. Podoprygorina, V. Böhmer, C. Rangan, S. Mittler, *Phys. Rev. B*, **2008**, *77*, 235446.
- [5] S.M. Hashemi Rafsanjani, T. Cheng, S. Mittler, C. Rangan, *J. Appl. Phys.* 2010, *107*, 094303.
- [6] M.D. Malinsky, K.L. Kelly, G.C. Schatz, R.P. van Duyne, *J. Am. Chem. Soc.* **2001**, *123*, 1471.
- [7] L.S. Jung, C.T. Campbell, T.M. Chinowsky, M.N. Mar, S.S. Yee, *Langmuir* **1998**, *14*, 5636.
- [8] S. Ekgasit, C. Thammacharoen, W. Knoll, *Anal. Chem.* **2004**, *76*, 561.
- [9] P. John, S.J. Moss, A. Ledwith, *In The Chemistry of the Semiconductor Industry*, Chapman and Hall: New York, **1987**.
- [10] U. Weckenmann, S. Mittler, S. Krämer, A.K.A. Aliganga, R.A. Fischer, *Chem.Mater.* **2004**, *16*, 621.
- [11] N.L. Jeon, W. Lin, M.K. Erhardt, G.S. Girolami, G.S., R.G. Nuzzo *Langmuir*, **1997**, *13*, 3833.
- [12] C. Thurier, P. Doppelt, *Coord. Chem. Rev.* **2008**, *252*, 155.
- [13] M. Brust, J. Fink, D. Bethell, D.J. Schiffrin, C. Kiely, *J. Chem. Soc., Chem. Commun.* **1995**, *16*, 1655.
- [14] R.G. Palgrave, I.P. Parkin, *Chem. Mater.* **2007**, *19*, 4639.
- [15] R.G. Palgrave, I.P. Parkin, *Gold Bulletin* **2008**, *41*, 66.
- [16] M. Saeli, R. Binions, C. Piccirillo, G. Hyett, I.P. Parkin, *Polyhedron* **2009**, *28*, 2233
- [17] Michael E.A. Warwick, Charles W. Dunnill, and Russell Binions, *Chem. Vap. Deposition* **2010**, *16*, 220.
- [18] A.K.A. Aliganga, I. Lieberwirth, G. Glasser, A. Duwez, Y. Sun, S. Mittler, *Org. Electron.* **2007**, *8*, 161.
- [19] E. Ertorer, J.C. Avery, L.C. Pavelka, S. Mittler, *Chem. Vap. Deposition* **2013**, *19*, 338.

- [20] G. Beamson, D. Briggs, *High Resolution XPS of Organic Polymers - The Scienta ESCA300 Database*, Wiley Interscience, **1992**.
- [21] D.B. Pedersen, E.J.S. Duncan, *Surface Plasmon Resonance Spectroscopy of Gold Nanoparticle- Coated Substrates* Technical Report DRDC Suffield TR **2005**, 109.
- [22] J.G. Ortega-Mendoza, A. Padilla-Vivanco, C.T.P.Z.D. Villegas-Hernández, F. Chávez, *Sensors* **2014**, *14*, 18701.
- [23] E. Ertorer, PhD Thesis, University of Western Ontario, **2013**.
- [24] L. Tang, R. Zhang, X. Zhou, M. Pan, M. Chen, X. Yang, P. Zhou, Z. Chen, *BioRes.*, **2012**, *7*, 3327.
- [25] A. Rezaee, K.K. Wong, T. Manifar, S. Mittler, *Surf. Interface Anal* **2009**, *41*, 615.
- [26] Springer, “*Modern Aspects of Electrochemistry*” (ed. M. Schlesinger), “*Experimental and Theoretical Issues of Nanoplasmonics in Medicine*”, D. Travo, R. Huang, T. Cheng, C. Rangan, E. Ertorer, S. Mittler, Volume 104 (2013) 343.
- [27] A. Battisti, O. Bellina, P. Diversi, S. Losi, F. Marchetti, P. Zanello, *Eur. J. Inorg. Chem.* **2007**, 865.